Dual Band Deep Ultraviolet AlGaN Photodetectors

S. Aslam, L. Miko, C. Stahle, D. Franz, D. Pugel, B. Guan, J. P. Zhang and R. Gaska

We report on the design, fabrication and characterization of a back-illuminated voltage bias selectable dual-band AlGaN UV photodetector. The photodetector can separate UV-A and UV-B band radiation by bias switching a two terminal *n-p-n* homojunction structure that is fabricated in the same pixel. When a forward bias is applied between the top and bottom electrodes, the detector can sense UV-A and reject UV-B band radiation. Alternatively, under reverse bias, the photodetector can sense UV-B and reject UV-A band radiation.

Introduction: Ultra-violet (UV) detectors are of great importance for aerosol remote sensing, UV dose monitoring, dermatology and numerous other applications that are cited widely in the literature. The UV spectrum is commonly classified into three regions, UV-A (315nm to 400nm), UV-B (280 nm to 315 nm) and UV-C (<280 nm). The atmospheric transmission efficiency drops drastically from UV-A to UV-C. Harmful UV-C radiation should be completely absorbed by the atmospheric ozone layer, but leakage due to ozone depletion is of great concern. The degrading influence on living organisms on the surface of Earth, especially on human beings, varies significantly from UV-A to UV-C. Thus, a multi-band UV detector and imaging array technology, which can detect and image multiple UV bands, would be highly desirable.

AlGaN UV detectors and imaging technologies have made rapid progress over the years [1,2,3]. One of the unique advantages of AlGaN wide bandgap semiconductors is that hetero-structures can be fabricated by tuning the stoichiometeric ratio of Al in AlGaN. As a result, an intrinsic band-pass filter can be formed using AlGaN *p-i-n* hetero-structures with appropriate Al ratio in different layers, which can eliminate the need for external visible blocking filters in many applications [3,4]. Also, the availability of AlGaN hetero-structures makes it feasible to fabricate multi-color UV detectors by stacking multiple junctions.

One technique for dual band detection is stacking two *p-n* structures back to back and forming a two terminal *n-p-n* homojunction structure [1]. Dual band detectors should be optimized for unity gain and the absorption in the center *p* region should be minimized. When a positive bias is applied between the top and bottom *n* layer, the top *n-p* junction is reverse biased, acting as a detector, and the bottom *p-n* junction is at forward bias, acting as a variable resistor. When the bias is flipped, the top *n-p* becomes a variable resistor and the bottom *p-n* junction becomes a detector. If the top and bottom detectors are judiciously designed to respond to different wavelengths then two different radiation bands can be sensed by switching the bias polarity across the detector. This technology has been successfully used to fabricate a two-color HgCdTe IR detector [1,5]. In this Letter, we present AlGaN UV detector with a *n-p-n* heterostructure, which can respond to UV-A and UV-B separately in the same pixel by switching the bias across the device.

Photodiode design: An *n-p-n* multi-layer AlGaN structure has been designed for UV-A and UV-B detection based on the energy bandgap equation given by Bougrov *et al.* [6],

$$E_g(x) = E_g(GaN)(1-x) + E_g(AlN)x - bx(1-x) \qquad (1)$$

where x is the Al molar fraction, $E_g(GaN) = 3.41\text{eV}$ and $E_g(AlN) = 6.2\text{eV}$ are the energy bandgaps for GaN and AlN at 300K and b (between 0eV to 1eV) is the bowing factor. By varying the $Al_xGa_{(1-x)}N$ stoichiometry the long wavelength cut-off can be manipulated. In the *n-p-n* dual band detector, there are five layers comprised of the n^+ top ohmic contact layer, the first absorber doped with n^- or p^-, the center p^+ layer, the second n^- or p^- absorber, and the n^+ for bottom ohmic contact. Since, the unintentional doping for AlGaN is *n* type and the minimum doping concentration of n^- layers can be controlled to be lower than that of p^- layer, n^- doping is preferred for the two absorber layers.

Fig. 1 shows a cross-sectional view of the detector showing the five distinct growth layers: (I) Si-doped n^+ layer, (II) Mg-doped p layer, (III) Mg doped p^+ layer, (IV) Mg-doped p layer and (V) Si doped n^+ layer with thickness' 0.05μm, 0.3μm, 0.1μm, 0.3μm and 1μm, respectively.

Photodiode fabrication and testing: The *n-p-n* detector mesa structure was defined by conventional photolithography utilizing Cl-based chemistry RIE etching. Electron beam evaporated Ni-Au bi-layer ohmic contacts were deposited on the top and bottom *n* layers followed by a rapid thermal anneal. The inset in Fig. 1 shows the top view of a fabricated 300μm diameter *n-p-n* dual band AlGaN detector. A and B denote the ohmic contact electrodes.

Fig. 2 shows the *I-V* characteristics measured with and without UV illumination using a Keithley 4200 semiconductor parameter analyzer. In the measurement, electrode A, connected to the bottom n^+ layer, is grounded and the bias on electrode B on the top is scanned from -10V to +10V. The bottom I-V curve is measured in the dark. It is seen that the leakage current is lower than 10^{-12} A between -10V and 5V. The detectors become

very leaky at biases above 5V and the leakage current increases rapidly from 5V to 10V. The rapid increase is attributed to the poor junction quality of the top n^+-p^+ junction formed by the memory effect of Mg [7].

Under 290 nm back illumination, the photocurrent is around $1x10^{-12}$A under small forward biases. Under reverse bias, the photocurrent increases from 0.7pA to 400pA from 1V to -1V. From -1V to -10V, the photocurrent increases slowly from 400pA to 3nA. Under 340nm UV illumination, the photocurrent is around 2pA under reverse bias conditions. From -1V to 1V, it rapidly increases from 0.5pA to more than 0.2nA and then increases to 6nA at 10V. As shown in Fig. 2, under reverse bias, the detector is active for 290nm and blind to 340nm. The ratio of the photo-response at 290 nm and 340 nm is over two orders of magnitude under reverse bias. Under forward bias, the detector is active to 340nm and blind to 290nm. The ratio of the photo-response at 340 nm and 290 nm is over three orders of magnitude under forward bias, indicating an excellent out-of-band rejection.

The external quantum efficiency was determined by comparing the photocurrent as a function of the incident power measured by Newport 1830-C power-meter with a calibrated Si photodiode. Fig. 3 shows the spectral quantum efficiency of a dual band UV detector with +5V and -5V applied on the top and the bottom being grounded. As shown in the figure, the detector at -5V has the cut-on and cut-off wavelength at 280 nm and 315 nm, respectively. The cut-on wavelength corresponds to the bandgap of the $Al_{0.2}Ga_{0.8}N$ absorber (layer IV) and the cut-off wavelength corresponds to the bandgap of the $Al_{0.47}Ga_{0.53}N$ (layer V). At +5V, the cut-on and cut-off wavelength of the response spectrum are 320nm and 360nm, determined by the bandgap of $Al_{0.2}Ga_{0.8}N$ (layer III and

IV) and the top GaN absorber (layer II). The peak quantum efficiency at +5V and -5V is 14% and 25%, respectively. At -10V, the peak quantum efficiency is over 65%. At +10V, the peak quantum efficiency is 23%. Since the leakage current becomes very high at +10V, the photocurrent cannot be determined accurately and thus the photo-response spectrum is not shown in this figure. Both response spectra show clearly the cut-off and cut-on wavelength. As can be seen, the out-of-band rejection is over two orders of magnitude.

Discussion: It is noted that the maximum quantum efficiency under forward bias is substantially lower than that under reverse bias. This can be explained by the difference of the doping levels for the two absorber layers. Due to the Mg memory effect, the doping level in GaN absorber (layer II) is much higher than that in $Al_{0.2}Ga_{0.8}N$ (Layer IV). The depletion width in GaN absorber is smaller than that in $Al_{0.2}Ga_{0.8}N$ under the same bias level. Consequently, the quantum efficiency under forward biasing is lower than that under reverse biasing. The asymmetric response spectra for UV-A and UV-B can be eliminated by suppressing the Mg memory effect during the material growth. The maximum quantum efficiency for UV-A can be significantly improved.

One of the advantages of the *n-p-n* type photo-detectors is its compatibility with most standard readout electronics designed for regular photodiodes. Two different UV bands can be monitored using one pixel and the readout electronics developed for single band UV detectors. A large format photodiode array can be developed using standard Si readout chips commercially available for photodiode arrays. The development of a dual band UV AlGaN detector has the advantage of sensing two UV bands without sacrificing the optical resolution and introducing aliasing for UV multi-band imaging.

However, since the structure contains two back-to-back *p-n* junctions, the linearity may become an issue. As the photocurrent increases, the voltage across the forward biased junction has to increase and the voltage across the reverse biased junction is therefore reduced. As a result, the depletion width decreases and the quantum efficiency drops. For the structure we have investigated, the photocurrent continued to increase as the bias increased, indicating that the absorber is not fully depleted even for a -10V bias. The linearity may not be good when the photocurrent is high but needs to be investigated further. This problem may be solved by controlling the Mg memory effect and the out-diffusion of Mg to make the doping of the n^- GaN and $Al_{0.2}Ga_{0.8}N$ absorbers low enough so that they are fully depleted at the operating bias voltage level.

It should also be pointed out that the same *n-p-n* structure can be designed to respond to two consecutive UV bands between 250nm and 365nm based on the current AlGaN growth technology. If the Al ratio in the center p^+ layer (layer III) is different from Al ratio in the bottom absorber (layer IV), the structure can be designed to respond to two different UV bands with the center wavelengths and the spectral resolution designable. The spectral resolution is only limited by the uniformity of the Al molar concentration.

Summary: An AlGaN dual band *n-p-n* photo-detector has been designed and fabricated. Under forward bias condition, the detector can selectively sense UV photons between 320 nm and 365 nm. The maximum external quantum efficiency at 10V is 23%. Under reverse bias condition, the detector responds to UV photons between 280 nm and 315 nm. The maximum external quantum efficiency at 10V is over 65%. The low quantum efficiency in UV-A is caused by the poor junction quality of the top p^+-n^+ junction

formed due to the Mg memory effect. It can be significantly improved by suppressing the Mg memory effect during the material growth.

Acknowledgements: S. Aslam, wishes to thank M. Ismail for enlightening discussions.

Authors' affiliations:

S. Aslam, L. Miko, C. Stahle, D. Franz, D. Pugel and B. Guan *(NASA/Goddard Space Flight Center, Detector Systems Branch, Code 553, Greenbelt, MD 20771)*

E-mail: saslam@pop200.gsfc.nasa.gov

J. P. Zhang and R. Gaska *(Sensor Electronic Technology, Inc., 1195 Atlas Rd., Columbia, SC 29209)*

References

1 M. A. Khan, J. N. Kuznia, D. T. Olson, M. Blasingame, and A. R. Bhattarrai, Appl. Phys. Lett. **63**, 2455 (1993).

2 J. P. Long, S. Varadaraajan, J. Mathews, and J. F. Schetzina, Opto-electronics Review **10**, 251 (2002).

3 P. Lamarre, A. Hairston, S. P. Tobin, K. K. Wong, A. K. Sood, M. B. Reine, M. Pophristic, R. Brikham, I. T. Ferguson, R. Singh, C. R. Eddy, Jr., U. Chowdhury, M. M. Wong, R. D. Dupiuis, P. K. Kozodoy, and E. J. Tarsa, phys. stat. sol. **188**, 289 (2001).

4 E. R. Blazejewski, J. M. Arias, G. M. Williams, W. Mclevige, and M. Zandian, J. Vac. Sci. Technol. B **10**, 1627 (1992).

5 E. P. Smith, L. T. Pham, G. M. Venzor, E. Norton, M. Newton, P. Goetz, V. Randall, G. Pierce, E. A. Patten, R. A. Coussa, K. Kosai, W. A. Radford, J. Edwards, S. M. Johnson, S. T. Baur, J. A. Roth, B. Nosho, J. E. Jensen, and R. E. Longshore, Proc. of SPIE **5209**, 1 (2003).

6 V. Bougrov, M. Levinshrein, S. Rumyantsev, A. Zubrilov, Book Chapter in "Properties of Advanced Semiconductor Materials: GaN, AIN, InN, BN, SiC, SiGe," Editors: M. E. Levinshtein, S. L. Rumyantsev, M. S. Shur, John Wiley & Sons, ISBN: 978-0-471-35827-5 (2001).

7 H. Xing, D. S. Green, H. J. Yu, T. Mates, P. Kozodoy, S. Keller, S. P. Denbaars, and U. K. Mishra, Jpn. J. Appl. Phys., Part I **42**, 50 (2003).

Fig. Captions:

Fig. 1. Cross-sectional view of *n-p-n* dual band detector structure. The inset is the top view picture of a 300μm diameter detector; A and B are the bottom and top electrodes.

Fig. 2. *I-V* characteristics of the *n-p-n* dual band detector showing UV-A and UV-B response as measured in the dark and under 340nm and 290nm UV illumination.

Fig. 3. Quantum efficiency versus wavelength of dual band detector showing UV-A and UV-B response with +5V, -5V and -10V bias.

Fig. 1. Aslam *et al.*

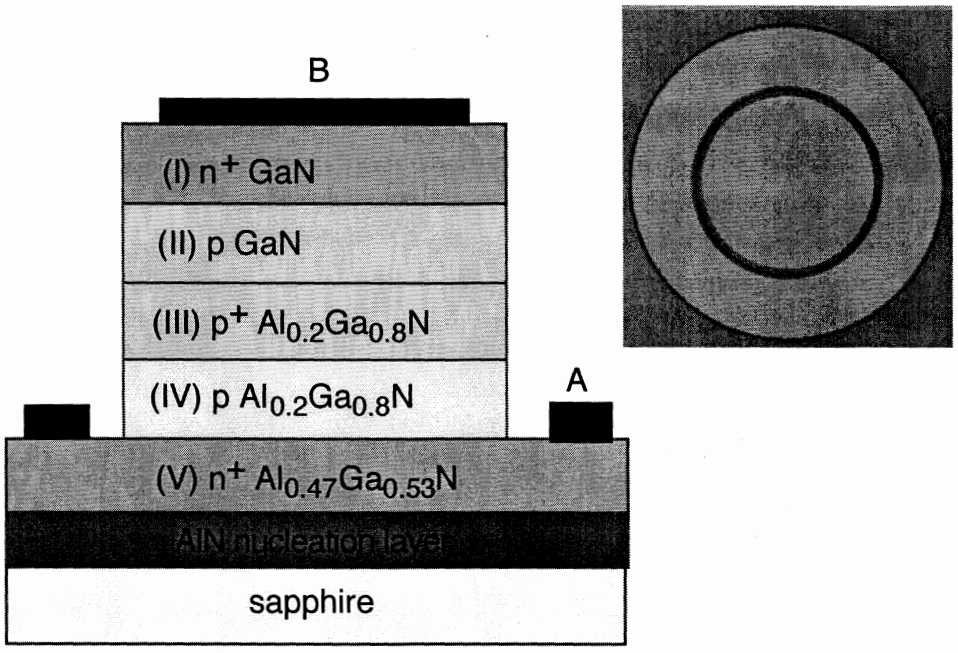

Fig. 2. Aslam *et al.*

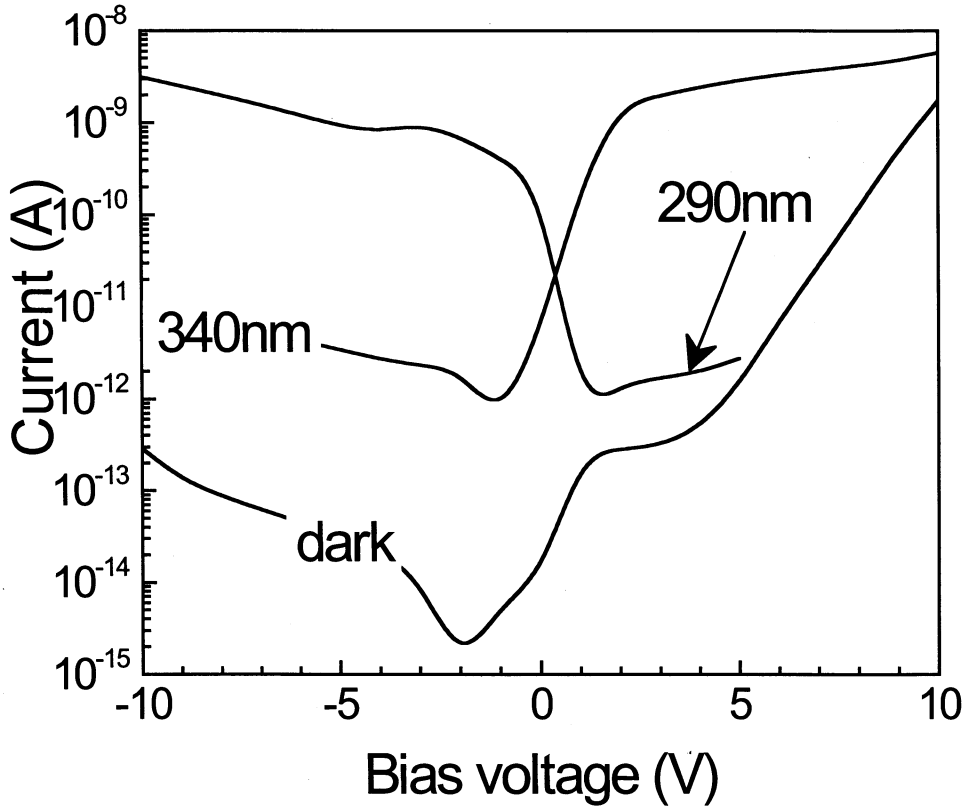

Fig. 3. Aslam *et al.*